OXFORD

SOT | Society of Toxicology
www.toxsci.oxfordjournals.org

TOXICOLOGICAL SCIENCES, 171(1), 2019, 1–12

doi: 10.1093/toxsci/kfz146
Advance Access Publication Date: June 26, 2019
Research Article

The Protective Roles of PPARα Activation in Triptolide-Induced Liver Injury

Dan-Dan Hu,[*,†,1] Qi Zhao,[*,1] Yan Cheng,[*,1] Xue-Rong Xiao,[*] Jian-Feng Huang,[*] Yan Qu,[*] Xian Li,[†] Ying-Mei Tang,[‡,2] Wei-Min Bao,[§] Jin-Hui Yang,[‡] Tao Jiang,[‡] Jia-Peng Hu,[¶] Frank J. Gonzalez,[‖] and Fei Li[*,2]

[*]State Key Laboratory of Phytochemistry and Plant Resources in West China, Kunming Institute of Botany, Chinese Academy of Sciences, Kunming 650201, China; [†]School of Pharmaceutical Science and Yunnan Key Laboratory of Pharmacology of Natural Products, Kunming Medical University, Kunming 650500, China; [‡]Department of Gastroenterology, Yunnan Research Center for Liver Diseases, The 2nd Affiliated Hospital of Kunming Medical University, Kunming 650033, China; [§]Department of General Surgery, Yunnan Provincial 1st People's Hospital, Kunming 650032, China; [¶]Clinical Laboratory, The 2nd Affiliated Hospital of Kunming Medical University, Kunming 650033, China; and [‖]Laboratory of Metabolism, National Cancer Institute, National Institutes of Health, Center for Cancer Research, Bethesda, Maryland 20892

[1]These authors contributed equally to this study.
[2]To whom correspondence should be addressed. Fax: +86-871-65216953. E-mail: lifeib@mail.kib.ac.cn and Fax: +86-871-63402288. E-mail: tangyingmei_med@163.com.

The authors certify that all research involving human subjects was done under full compliance with all government policies and the Helsinki Declaration.

ABSTRACT

Triptolide (TP), one of the main active ingredients in *Tripterygium wilfordii* Hook F, is clinically used to treat immune diseases but is known to cause liver injury. The aim of this study was to investigate the biomarkers for TP-induced hepatotoxicity in mice and to determine potential mechanisms of its liver injury. LC/MS-based metabolomics was used to determine the metabolites that were changed in TP-induced liver injury. The accumulation of long-chain acylcarnitines in serum indicated that TP exposure disrupted endogenous peroxisome proliferator-activated receptor α (PPARα) signaling. Triptolide-induced liver injury could be alleviated by treatment of mice with the PPARα agonist fenofibrate, whereas the PPARα antagonist GW6471 increased hepatotoxicity. Furthermore, fenofibrate did not protect *Ppara*−/− mice from TP-induced liver injury, suggesting an essential role for the PPARα in the protective effect of fenofibrate. Elevated long-chain acylcarnitines may protect TP-induced liver injury through activation of the NOTCH-NRF2 pathway as revealed in primary mouse hepatocytes and *in vivo*. In agreement with these observations in mice, the increase in long-chain acylcarnitines was observed in the serum of patients with cholestatic liver injury compared with healthy volunteers. These data demonstrated the role of PPARα and long-chain acylcarnitines in TP-induced hepatotoxicity, and suggested that modulation of PPARα may protect against drug-induced liver injury.

Key words: liver injury; metabolomics; PPARα; acylcarnitines.

Tripterysium glycoside tablets derived from *Tripterygium wilfordii* Hook F have long been used for the treatment of autoimmune diseases in clinical practice. Triptolide (TP), one of the major bioactive diterpenes in tripterysium glycosides tablets, is most noted for its anti-inflammatory, immunosuppressive (Liu *et al.*, 2005), anti-fertility (Matlin *et al.*, 1993), anticancer

(Yang *et al.*, 2003), and antirheumatic (Tao *et al.*, 2001). However, clinical use of TP is limited because of its toxicity to liver, kidney, spleen, and heart.

Liver injury in acute and chronic conditions may be induced by drugs, toxic xenobiotics, viral hepatitis, and multiple heritable gene mutations. Patients with suspected liver damage are initially subjected to liver function tests that include the assessment of serum aspartate aminotransferase (AST), alanine aminotransferase (ALT), and alkaline phosphatase (ALP) levels. If the levels of these enzymes are abnormal, patients could be subjected to biopsy which is the gold standard used to diagnose liver injury (Soga *et al.*, 2011). Therefore, development of novel diagnostic biomarker with greater sensitivity would enhance the efficiency in the diagnosis of liver damage. Previous studies found serum acylcarnitine levels can provide a better prediction to monitor the initiation of drug-induced hepatotoxicity compared with traditional diagnosis with serum ALT, AST, and ALP (Chen *et al.*, 2009; McGill *et al.*, 2014). Clinically, acylcarnitine levels were used as diagnostic markers of inherited diseases, including carnitine palmitoyltransferase 1 (CPT1) deficiency, medium-chain acyl-CoA dehydrogenase deficiency, very-long-chain acyl-CoA dehydrogenase deficiency, and CPT2 deficiency (Santra and Hendriksz, 2010). Interestingly, these defective genes were direct or indirect peroxisome proliferator-activated receptor α (PPARα) target genes (Mandard *et al.*, 2004). A previous study demonstrated that acetaminophen (APAP) treatment can cause the accumulation of serum acylcarnitines through suppression of PPARα (Chen *et al.*, 2009). In addition, activation of PPARα by fenofibrate can reduce the accumulation of acylcarnitines in mice administered cocaine and α-naphthylisothiocyanate (Shi *et al.*, 2012; Zhao *et al.*, 2017). Therefore, serum long-chain acylcarnitines may be a potential diagnostic biomarker for liver injury, and the activation of PPARα may be considered as a therapeutic target of liver injury.

In this study, the protective role of PPARα and long-chain acylcarnitines in hepatotoxicity was determined after TP exposure using ultra-performance chromatography electrospray ionization quadrupole time-of-flight mass spectrometry (UPLC-ESI-QTOFMS)-based metabolomics. LC/MS-based metabolomics has been widely used for identifying the metabolic pathways associated with hepatotoxicity and renal toxicity (Chen *et al.*, 2016, 2017; Li *et al.*, 2012; Zhang *et al.*, 2012; Zhao *et al.*, 2018). This study revealed that TP could inhibit PPARα signaling and that PPARα activation by fenofibrate could significantly attenuate TP-induced liver injury. Long-chain acylcarnitines were found to be a liver injury biomarker and to protect liver injury through the NOTCH-NRF2 pathway. More importantly, cholestatic liver injury in patients also showed the accumulation of serum long-chain acylcarnitines. These findings provide important insights into the protective role of PPARα activation and long-chain acylcarnitines in TP-induced liver injury, and suggest that activation of PPARα may protect against clinical liver injury.

MATERIALS AND METHODS

Chemicals and reagents. Triptolide and fenofibrate were obtained from Chengdu Mansite Bio-technology Co Ltd (Chengdu, China). GW6471, formic acid, chlorpropamide, lauroylcarnitine (12:0-carnitine), myristoylcarnitine (14:0-carnitine), palmitoylcarnitine (16:0-carnitine), and stearoylcarnitine (18:0-carnitine) were purchased from Sigma-Aldrich (St. Louis, Missouri). N-[N-(3,5-difluorophenacetyl)-L-alanyl]-S-phenylglycine t-butyl ester (DAPT) was obtained from Medchemexpress (Monmouth Junction, New Jersey). All organic reagents were of the highest grade commercially available.

Patients. A total of 36 serum samples were obtained from The Second Affiliated Hospital of Kunming Medical University. Eighteen patients were diagnosed with cholestatic liver injury and 18 healthy volunteers aged from 32 to 62 years were involved in this study. The health of all volunteers was assessed by clinicians before and during the study. Informed consent was obtained from all individual participants involved in the study. The study protocol conformed to the ethical guidelines of the 1975 Declaration of Helsinki as reflected in *a priori* approval by the institution's human research committee (The Second Affiliated Hospital of Kunming Medical University, registration number: PJ-2017-25). Clinical characteristics of patients, found in Supplementary Table 1, were measured using the VetScan VS2 Comprehensive Diagnostic Profile (Abaxis, Inc, Union City California).

Animals and treatment. Animal experiments were approved by the institutional ethical committee of Kunming Institute of Botany. Male C57BL/6J mice (6–8 weeks old) were purchased from Slaccas Laboratory Animal Co, Ltd (Hunan, China). Male wild-type (*Ppara*+/+) and *Ppara*-null (*Ppara*−/−) mice (6–8 weeks old) on the 129/Sv genetic background was previously described in Chen *et al.* (2009). The mice were maintained under a standard light/dark of 12 h/12 h cycle and humidity 50%–60% with water and standard rodent chow *ad libitum*.

Experiment 1: To find the biomarker of TP-induced liver injury, the C57BL/6J mice were given a single intraperitoneal injection of TP (1.0 mg/kg dissolved in 1% DMSO water solution, $n = 4$). All mice were killed after TP administration for 18 h. Serum and liver samples were collected and stored at −80°C until analysis.

Experiment 2: To investigate the protective effect of PPARα on TP-induced liver injury, the *Ppara*+/+ and *Ppara*−/− mice in 129/Sv genetic background were randomly assigned into 3 groups, respectively ($n = 5$): (1) control; (2) TP; (3) Fenofibrate+TP. Fenofibrate+TP group was orally treated with fenofibrate (200 mg/kg dissolved in 0.5% sodium carboxymethylcellulose) for 3 consecutive days before TP treatment (Zhao *et al.*, 2017). Triptolide and Fenofibrate+TP groups were given a single dose of TP. All mice were killed 18 h after TP administration. Serum and liver samples were collected and stored at −80°C until analysis.

Experiment 3: To determine the role of PPARα on metabolism of TP, *Ppara*+/+ and *Ppara*−/− mice on the 129/Sv genetic background and fenofibrate treatment were used ($n = 5$): (1) TP (*Ppara*+/+); (2) TP (*Ppara*−/−); (3) Fenofibrate+TP (*Ppara*+/+). Fenofibrate+TP group (*Ppara*+/+) was orally treated with 200 mg/kg fenofibrate for 3 consecutive days before 1 mg/kg TP treatment. Triptolide (*Ppara*+/+), TP (*Ppara*−/−), and Fenofibrate+TP (*Ppara*+/+) groups were given a single IP dose of TP. All the experimental mice were housed separated in metabolic cages for 18 h. Urine and feces were collected for a period of 1–18 h, and serum samples were harvested at 15 min and 18 h after TP administration. All samples were stored at −80°C until analysis.

Experiment 4: To investigate the role of PPARα antagonist, GW6471, in TP-induced liver injury, the C57BL/6J mice were randomly assigned into 3 groups ($n = 5$): (1) control; (2) TP; (3) GW6471+TP. GW6471+TP group was treated with GW6471 (10 mg/kg dissolved in 4% Tween 80 saline solution, IP) for 3 consecutive days before TP treatment (Zhao *et al.*, 2017). The TP and

GW6471+TP groups were given a single dose of TP. All mice were killed after TP administration for 18 h. Serum and liver samples were collected and stored at −80°C until analysis.

Experiment 5: For study with incremental doses of TP, the C57BL/6J mice were treated with 0.5, 0.8, and 1 mg/kg TP. All mice were killed after TP administration for 18 h. Serum sample was collected and stored at −80°C until analysis.

Experiment 6: For study with time-effect and liver regeneration of TP, the C57BL/6J mice were randomly assigned into 2 groups ($n = 40$): (1) TP; (2) Fenofibrate+TP. Triptolide group was intraperitoneally treated with 1 mg/kg TP, and sacrificed at 0, 3, 6, 12, 18, 24, 48, 72 h after TP treatment. Fenofibrate+TP group was orally treated with 200 mg/kg fenofibrate for 3 consecutive days before 1 mg/kg TP treatment, and sacrificed at 0, 3, 6, 12, 18, 24, 48, 72 h after TP treatment.

Experiment 7: To evaluate the role of 18:0-carnitine in TP-induced liver injury, the C57BL/6J mice were randomly assigned into 3 groups ($n = 7$): (1) control; (2) TP; (3) TP + 18:0-carnitine. Triptolide + 18:0-carnitine group was treated with a single dose of 18: 0-carnitine (20 mg/kg dissolved in ethanol/Tween 80/water [1:1:10], IP, 30 min prior to TP treatment) (Gongora *et al.*, 2000). Triptolide and TP + 18:0-carnitine groups were given a single dose of TP. All mice were killed after TP administration for 18 h. Serum samples were collected and stored at −80°C until analysis.

Experiment 8: DAPT is a γ-secretase inhibitor, which can block NOTCH signaling by preventing the final cleavage step of the precursor form of NOTCH to the active NOTCH intracellular domain (NICD) (Jiang *et al.*, 2017). To evaluate the role of NOTCH pathway in TP-induced liver injury, the C57BL/6J mice were randomly assigned to 3 groups ($n = 7$): (1) control; (2) TP; (3) TP+DAPT. The TP+DAPT group was treated with a single dose of DAPT (10 mg/kg dissolved in DMSO, IP, 30 min prior to TP treatment) (Jiang *et al.*, 2017). Triptolide and TP+DAPT groups were given a single dose of TP. All mice were killed after TP administration for 24 h to evaluate survival rates. Serum samples (18 h) were collected and stored at −80°C until analysis.

Histological examination and biochemical assay. To assess liver damage, fresh liver samples were fixed in 10% neutral buffered formalin. Sections were stained with hematoxylin and eosin (H&E). Aspartate aminotransferase, ALT, and ALP activities were measured following manufacturer's instructions (Nanjing Jiancheng Bioengineering Institute, Nanjing, China).

Metabolomics analysis and data processing. Serum samples used for metabolomics were prepared using the method previously described in Zhao *et al.* (2017). The UPLC system was Agilent equipment consisting of a reverse-phase XDB-C18 column (2.1 × 100 mm, 1.8 μm, Agilent, Santa Clara, California). The liquid flow rate was 0.3 ml/min. (A) mobile phase was 0.01% formic acid in water, and (B) mobile phase was 0.01% formic acid in acetonitrile. The elution gradient was as follows: 0.0–12.0 min, 2%–98% B; 12.0–14.0 min, 98% B; 14.0–16.0 min, 98%–2% B. The column temperature was kept at 45°C, and the data were collected in the positive ion mode with electrospray ionization. Nitrogen was applied as both collision gas and drying gas. Capillary voltage was 3.5 kV. Drying gas temperature was 350°C, and nebulizer pressure was 35 psi. Five micromolar chlorpropamide was used as the internal standard.

MassHunter Workstation Software (Agilent) was used to the chromatographic and spectral data analysis. The data matrix was generated using Mass Profinder software (Agilent), and all data were normalized to peak areas of the internal standards. Then the data matrix was analyzed by SIMCA-P + 13.0 software (Umetrics, Kinnelon, New Jersey) for principal component analysis (PCA).

Xenobiotic metabolite analysis. Fifteen minutes serum samples or 18 h urine samples were prepared through mixing the 40 μl serum or 80 μl urine with 360 μl ethyl acetate containing 5 μM chlorpropamide. After vortexed for 1 min, the samples were centrifuged at 15 000 rpm for 5 min. Then, 300 μl supernatants were dried by N2 at room temperature. Subsequently, the residue was dissolved in 100 μl methanol. After centrifugation at 15 000 rpm for 20 min, 5 μl supernatants were injected into LC/MS.

Feces samples were prepared through mixing the 50 mg feces with 400 μl ethyl acetate containing 5 μM chlorpropamide. After shaking at room temperature for 20 min, the samples were centrifuged at 15 000 rpm for 5 min. Then, 150 μl supernatants were dried by N2 at room temperature. Subsequently, the residue was dissolved in 100 μl methanol. After centrifugation at 15 000 rpm for 20 min, 5 μl supernatants were injected into LC/MS.

RT-qPCR analysis and Western blot analysis. Total liver RNA was extracted from frozen tissues using Trizol reagent (Lifetechnologies, Carlsbad, California). qPCR was carried out in a CFX Connect Real-Time System (Bio-Rad Laboratories, Hercules, California) with SYBR green PCR master mix (TaKaRa, Dalian, China). The results were normalized to *Gapdh* mRNAs. qPCR primer sequences are listed in Supplementary Table 2. Western blot analyses were carried as detailed in a previous report (Crespillo *et al.*, 2011). The following antibodies were used: NOTCH3 (abs136713, ABSIN, Shanghai, China), NRF2 (D1Z9C, Cell Signaling Technology, Massachusetts), GAPDH (14C10, Cell Signaling Technology), and anti-rabbit peroxidase-conjugated second antibody (SA00001-2, Proteintech, Illinois).

Primary mouse hepatocytes isolation and culture. Primary mouse hepatocytes were isolated and cultured from male C57BL/6J mice using 2-step perfusion method (Li *et al.*, 2015). Cells were harvested after incubation with 18:0-carnitine (75 and 150 μM) for 18 h (Primassin *et al.*, 2008). The incubations were conducted in triplicates.

HepG2 cell culture. HepG2 was maintained in 1640 containing 10% fetal bovine serum. Cell were incubation with 12:0-carnitine, 14:0-carnitine, 16:0-carnitine, and 18:0-carnitine (20 and 100 μM) for 18 h.

Statistical analysis. All values were expressed as mean ± SEM. GraphPad Prism v.6 (GraphPad Software, Inc, San Diego, California) was applied for statistical analysis. p Value less than 0.05 was considered to be statistically significant.

RESULTS

Increased Serum Long-chain Acylcarnitines and Inhibition of PPARα in TP-induced Liver Injury

Hepatic histological and biochemical analysis showed that TP exposure dramatically increased hepatic congestion and AST, ALT, and ALP levels (Figs. 1A and 1B), indicating severe liver injury induced by TP. To further explore biomarkers of TP-induced liver injury, serum samples were examined by LC/MS-based metabolomics. The TP group deviated from the control

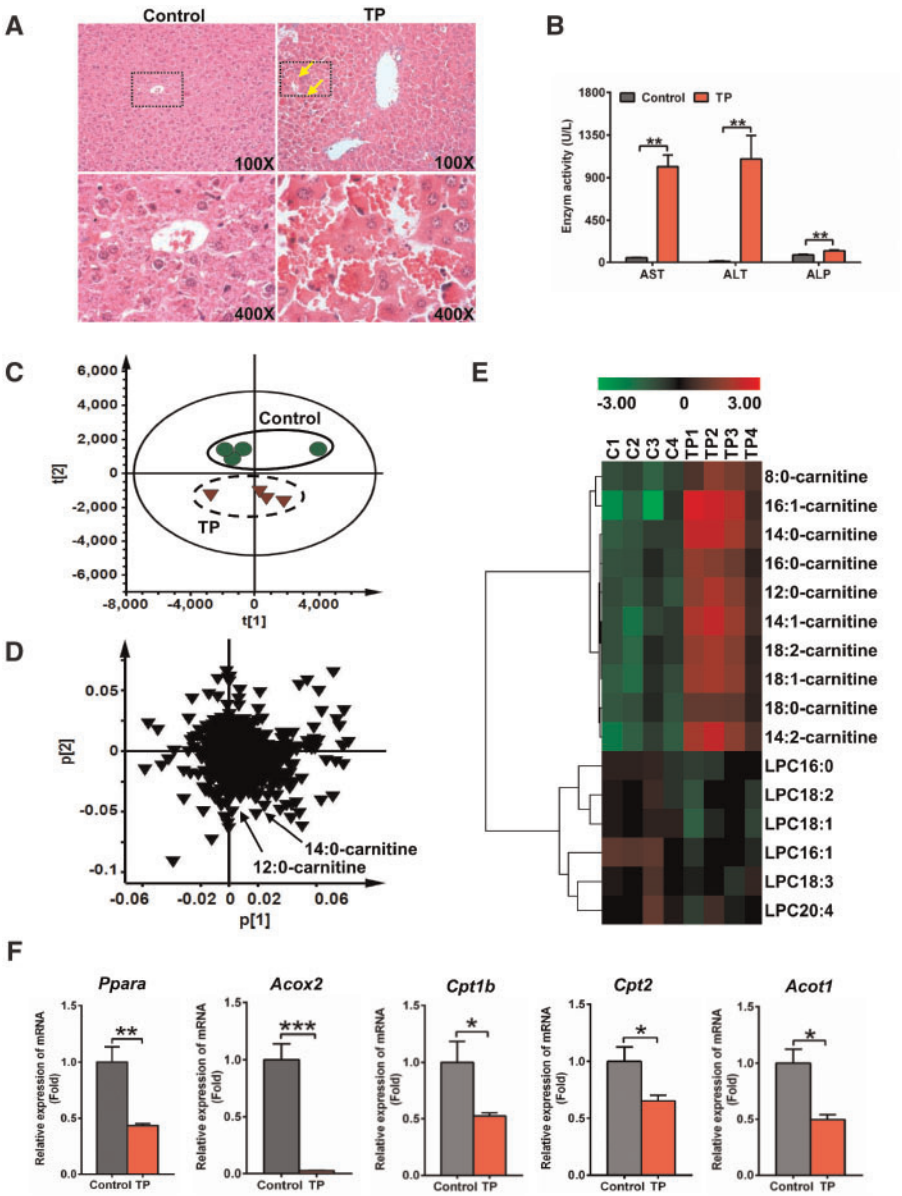

Figure 1. Triptolide (TP)-induced severe liver injury and inhibited peroxisome proliferator-activated receptor α signaling. A, Hematoxylin and eosin staining of liver. Solid arrow: congestion. B, Serum AST, ALT, and ALP enzymes activity. Principal component analysis score plot (C) and loading plot (D) derived from UPLC-QTOFMS data of serum ions. Each point represented an individual mouse serum sample (-top) and an ion in the sample (-bottom). Metabolites were labeled in the loading plot (●, control group; ▼, TP group). E, Heat map analysis of the relative abundance of medium- and long-chain acylcarnitines and LPCs in serum of control and TP groups. F, qPCR analysis was performed to measure the expression of *Ppara* mRNA and its target gene mRNAs (*Acox2*, *Cpt1b*, *Cpt2*, and *Acot1*). All data were expressed as mean ± SEM ($n = 4$). $^{*}p < .05$, $^{**}p < .01$, and $^{***}p < .001$.

group in PCA, indicating that TP dramatically altered the chemical composition of serum (Figure 1C). Two ions *m/z* 344.2794^{+} and 372.3107^{+} were found to deviate from the ions cloud in the loading scatter plot (Figure 1D). The MS/MS fragmentation identified these ions, *m/z* 344.2794^{+} (Rt = 8.43 min) and 372.3107^{+} (Rt = 9.38 min), as 12:0-carnitine and 14:0-carnitine, respectively. Target analysis showed that 10 medium- and long-chain acylcarnitines were significantly increased by TP ($p < .05$) (Figure 1E). Furthermore, long-chain acylcarnitines levels were increased within 2 h after TP treatment (Supplementary Figure 1). Further analysis revealed that the levels of long-chain acylcarnitines were positively correlated with the levels of AST and ALT ($p < .001$), which were 2 widely used markers for liver injury (Supplementary Figure 2).

Peroxisome proliferator-activated receptor α is the key regulator of fatty acid catabolism and thus modulates acylcarnitines levels. Thus, *Ppara* mRNA and its target gene mRNAs (acyl-CoA oxidase 2 [*Acox2*], *Cpt1b*, *Cpt2*, and Acyl-CoA thioesterase 1 [*Acot1*]) were measured in liver. *Ppara*, *Acox2*, *Cpt1b*, *Cpt2*, and *Acot1* mRNAs were significantly downregulated after TP treatment ($p < .05$) (Figure 1F), indicating inhibition of PPARα signaling by TP exposure. Taken together, these data indicated that TP exposure induced liver injury, accompanied with increased long-chain acylcarnitines that result from inhibition of PPARα signaling.

A dose-response study showed that TP-induced hepatotoxicity and acylcarnitine levels were gradually increased (Supplementary Figure 3). Triptolide-induced hepatotoxicity and acylcarnitine

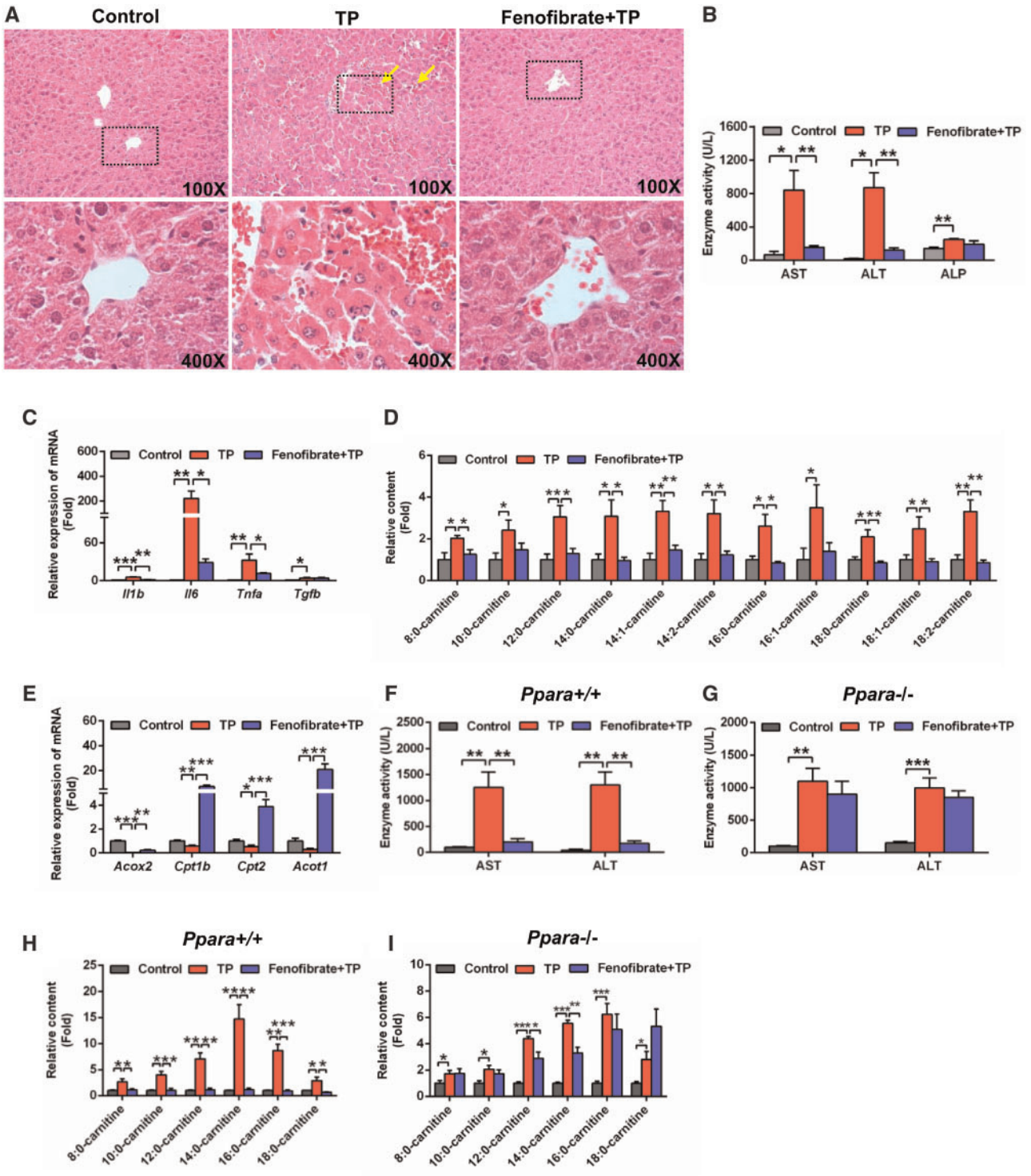

Figure 2. Fenofibrate attenuated TP-induced liver injury. A, Hematoxylin and eosin staining of liver. Solid arrow: congestion. B, Serum AST, ALT, and ALP enzymes activity. C, qPCR analysis of inflammatory factor mRNAs in liver. D, Fenofibrate recovered the increased serum medium- and long-chain acylcarnitine levels. E, qPCR analysis was performed to measure the expression of peroxisome proliferator-activated receptor α target gene mRNAs. Serum AST and ALT activity in *Ppara*+/+ mice (F) and *Ppara*−/− mice (G). Serum medium- and long-chain acylcarnitine levels in *Ppara*+/+ mice (H) and *Ppara*−/− mice (I). All data were expressed as mean ± SEM ($n = 5$). $^{*}p < .05$, $^{**}p < .01$, and $^{***}p < .001$.

levels were gradually increased within 24 h, and then decreased from 24 to 72 h (Supplementary Figs. 4A–F). Messenger RNAs encoding proliferating cell nuclear antigen (*Pcna*) and *Cyclin D1* (*Ccnd1*), 2 markers of cell proliferation and liver repair (Bhushan *et al.*, 2014, 2017) were measured after TP administration. *Pcna* and *Ccnd1* mRNAs were markedly induced 18–48 h after TP treatment, and their levels decreased after 48 h (Supplementary Figs. 4G and 4H). However, activation of PPARα by fenofibrate did not affect cell proliferation and liver repair during TP-induced toxicity (Supplementary Figs. 4G and 4H).

Activation of PPARα by Fenofibrate Ameliorated TP-induced Liver Injury

Because PPARα signaling was inhibited in TP-induced liver injury, activation of PPARα by fenofibrate might protect the mice from TP-induced liver damage. As expected, hepatic histological analysis showed that fenofibrate alleviated congestion induced by TP (Figure 2A). The elevations of AST and ALT in TP-induced liver injury were attenuated by fenofibrate (Figure 2B). In addition, fenofibrate treatment decreased the increased inflammatory cytokines interleukin-1β (*Il1b*), *Il6*, tumor necrosis factor α ($p < .05$) mRNAs after TP treatment (Figure 2C).

Serum metabolomics analysis indicated that the Fenofibrate+TP group was similar to the control group compared with the TP group (Supplementary Figure 5A). In the loading scatter plot of PCA, the 3 top increased ions 344.2794^+ (Rt = 8.43), 372.3107^+ (Rt = 9.38), and 428.3733^+ (Rt = 11.28) in the serum of TP group were identified as 12:0-carnitine, 14:0-carnitine, and 18:0-carnitine, respectively (Supplementary Figure 5B). Further target analysis showed that fenofibrate recovered the levels of 9 medium- and long-chain acylcarnitines (Figure 2D). The lower expression of *Acox2*, *Cpt1b*, *Cpt2*, and *Acot1* mRNA in TP-induced liver damage was recovered by fenofibrate (Figure 2E). These data suggested that PPARα activation ameliorated TP-induced liver injury.

To further determine the role of PPARα in TP-induced liver injury, *Ppara*−/− mice were treated with TP and Fenofibrate+TP. The decreased AST, ALT, and medium- and long-chain acylcarnitines levels in *Ppara*+/+ mice by fenofibrate were not observed in the *Ppara*−/− mice (Figs. 2F–I). These findings verified that PPARα played an important role in the therapeutic effect of fenofibrate.

To determine the role of PPARα on TP metabolism, *Ppara*−/− mice and fenofibrate treatment were used. The parent TP and its 3 hydroxylated metabolites were found in serum 15 min after administration (Supplementary Figure 6B). Three hydroxylated metabolites and a dihydroxylated metabolite were found in urine (Supplementary Figure 6C). No metabolites were detected in feces. These metabolites were identified in a previous report (Hu *et al.*, 2018). No obvious metabolic difference was found between *Ppara*+/+ mice and *Ppara*−/− mice, and there was no obvious metabolic difference in *Ppara*+/+ mice treated with fenofibrate compared with no vehicle treatment (Supplementary Figure 6). These results suggested that the change of PPARα status did not affect TP metabolism.

Inhibition of PPARα by GW6471 Aggravated TP-induced Liver Injury

Conversely, TP-induced liver injury was significantly increased by using a selective PPARα inhibitor, GW6471. Hematoxylin and eosin staining showed more congestion accompanied by higher ALT levels in the GW6471+TP group compared with the TP group ($p < .05$) (Figs. 3A and 3B). The levels of AST, ALP, and inflammatory cytokines were also slightly increased, although no significance was noted (Figs. 3B and 3C).

Serum metabolomics analysis showed that the GW6471+TP group was more deviated from control group compared with TP group (Supplementary Figure 7A), indicating that GW6471 treatment increased the toxicity of TP. In addition, long-chain acylcarnitines were significantly increased in the GW6471+TP group (Supplementary Figure 7B and Figure 3D). Finally, inhibition of *Cpt2* mRNA, encoded by a PPARα target gene, after treatment with GW6471 was also found (Figure 3E). These data demonstrated that inhibition of PPARα by GW6471 increased TP-induced liver injury.

Long-Chain Acylcarnitines Activated NOTCH-NRF2 Signaling Pathway

NOTCH signaling pathway could regulate development, differentiation, and homeostasis through cell-cell communication, which was associated with oxidative stress (Yaligar *et al.*, 2016). It has been demonstrated that there was a cross-talk between NOTCH3 and NRF2 pathways (Wakabayashi *et al.*, 2015). qPCR and WB analysis indicated that NOTCH-NRF2 pathway was activated by TP exposure (Figs. 4A–C), suggesting the increase in oxidative stress in TP-induced liver toxicity. Fenofibrate reduced the elevated expression of *Nrf2*, glutathione peroxidase 1 (*Gpx1*), *Gpx2*, *Gpx3*, *Gpx4*, *Notch1*, *Notch3*, and *Hes1* mRNAs induced by TP (Figs. 4A and 4B). Furthermore, the elevated protein levels of NRF2 and NOTCH3 were also recovered following the activation of PPARα by fenofibrate (Figure 4C).

The bioactivity of 12:0-carnitine, 14:0-carnitine, 16:0-carnitine, and 18:0-carnitine was evaluated in HepG2 cells. 18:0-Carnitine showed the strongest NRF2 activation compared with the other acylcarnitines (Supplementary Figure 8). Therefore, 18:0-carnitine was chosen for use in the following study. Expression of *Nrf2*, *Notch1*, *Notch2*, *Notch3*, and their target gene mRNAs *Gpx1*, *Gpx4*, *Gsta4*, and NOTCH-regulated ankyrin repeat protein (*Nrarp*), were dramatically increased following 18:0-carnitine exposure (Figs. 4D and 4E), suggesting that the increased long-chain acylcarnitines during liver injury would activate NRF2-NOTCH pathway.

Acylcarnitine-NOTCH Signaling Pathway Protected TP-Induced Liver Injury

To evaluate the important role of long-chain acylcarnitines, mice were treated with 20 mg/kg 18:0-carnitine. Hepatic histological analysis showed that 18:0-carnitine alleviated congestion induced by TP (Figure 5A). The elevations of AST, ALT, and medium- and long-chain acylcarnitines in TP-induced liver injury were attenuated by 18:0-carnitine treatment (Figs. 5B and 5C).

Mice treated with DAPT, which can block NOTCH signaling, showed increased congestion, mortality, and ALP levels (Figs. 5D–F). These results indicate that the inhibition of NOTCH signaling increased TP-induced liver injury. In summary, acylcarnitine-NOTCH signaling protected from TP-induced liver injury through defense response.

PPARα and Long-Chain Acylcarnitines in Cholestatic Liver Injury Patients

The cholestatic patients deviated from the normal subjects in PCA, indicating that cholestasis dramatically altered the chemical composition of serum (Figure 6A). Long-chain acylcarnitines were significantly increased in the cholestatic patients (Figs. 6B and 6C). Further analysis revealed that the levels of 18:0-carnitine were positively correlated with the levels of AST and ALT ($p < .001$) (Figure 6D). These findings demonstrated that PPARα and long-chain acylcarnitines played an important role in human liver injury.

DISCUSSION

Metabolomics analysis revealed that serum long-chain acylcarnitines could be used as diagnostic biomarker for liver injury and could also induce a defense response through activating the NOTCH-NRF2 pathway. Furthermore, activation of PPARα by fenofibrate could improve TP-induced liver injury. A clinical pilot study found that liver injury patients also had higher serum long-chain acylcarnitines and lower hepatic PPARα protein

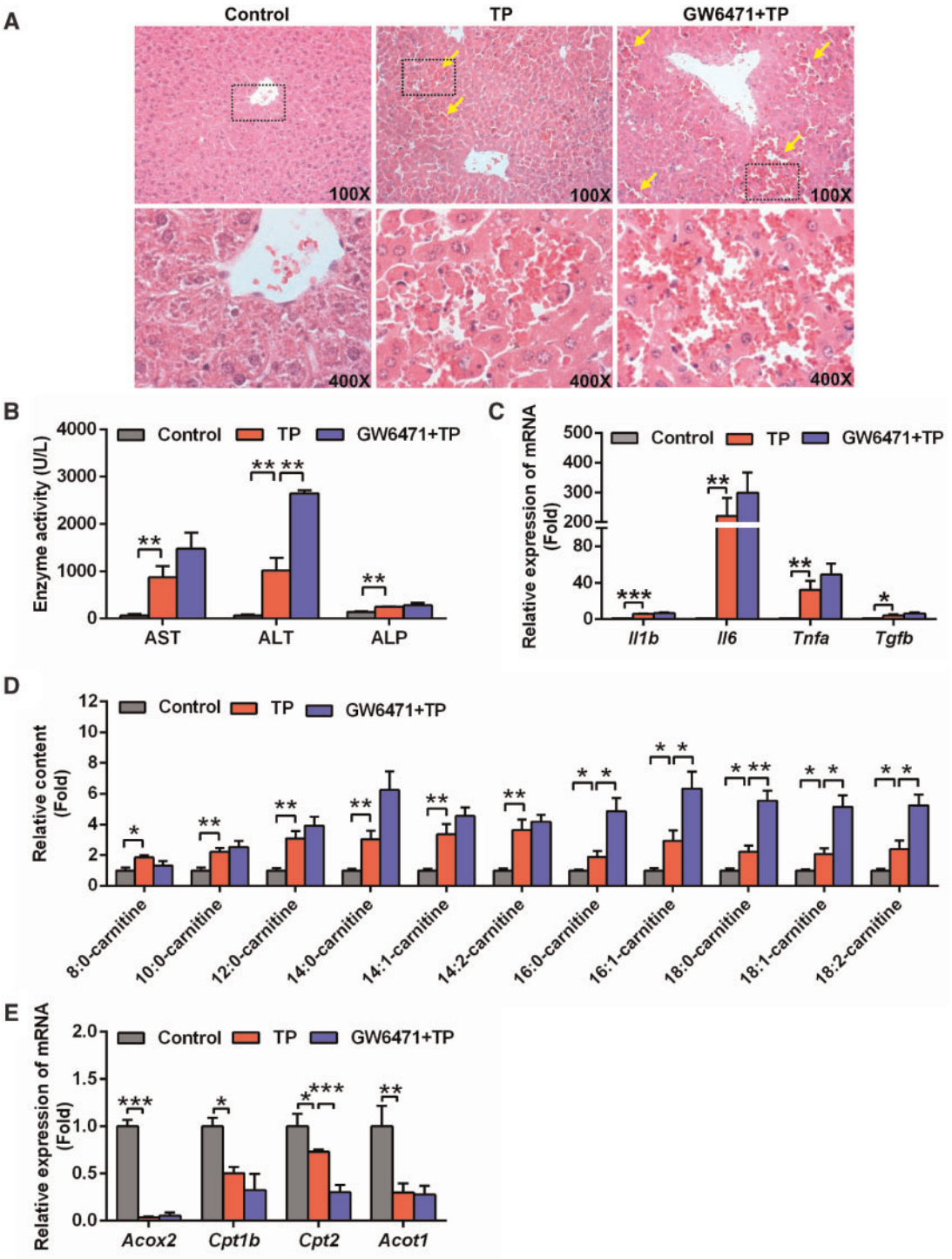

Figure 3. GW6471 aggravated TP-induced liver injury. A, Hematoxylin and eosin staining of liver. Solid arrow: congestion. B, Serum AST, ALT, and ALP enzymes activity. C, qPCR analysis of inflammatory factor mRNAs in liver. D, GW6471 aggravated the long-chain acylcarnitine levels in serum compared with TP group. E, QPCR analysis was performed to measure the expression of peroxisome proliferator-activated receptor α target gene mRNAs. All data were expressed as mean ± SEM ($n = 5$). $^{*}p < .05$, $^{**}p < .01$, and $^{***}p < .001$.

levels compared with healthy volunteers. These findings provide the rationale for the use of long-chain acylcarnitines as diagnostic biomarkers for liver injury, and PPARα agonists as therapeutic alternatives for liver injury.

The levels of acylcarnitines in serum have been used as clinical biomarkers for screening inborn genetic defects in fatty acid β-oxidation pathways (Santra and Hendriksz, 2010). Except for their association with genetic defects, acylcarnitines usually result from liver injury. The concentration of acylcarnitines was significantly higher in human hepatocellular carcinoma patients and in mice with liver tumors compared with normal subjects and non-tumor bearing mice (Yaligar *et al.*, 2016).

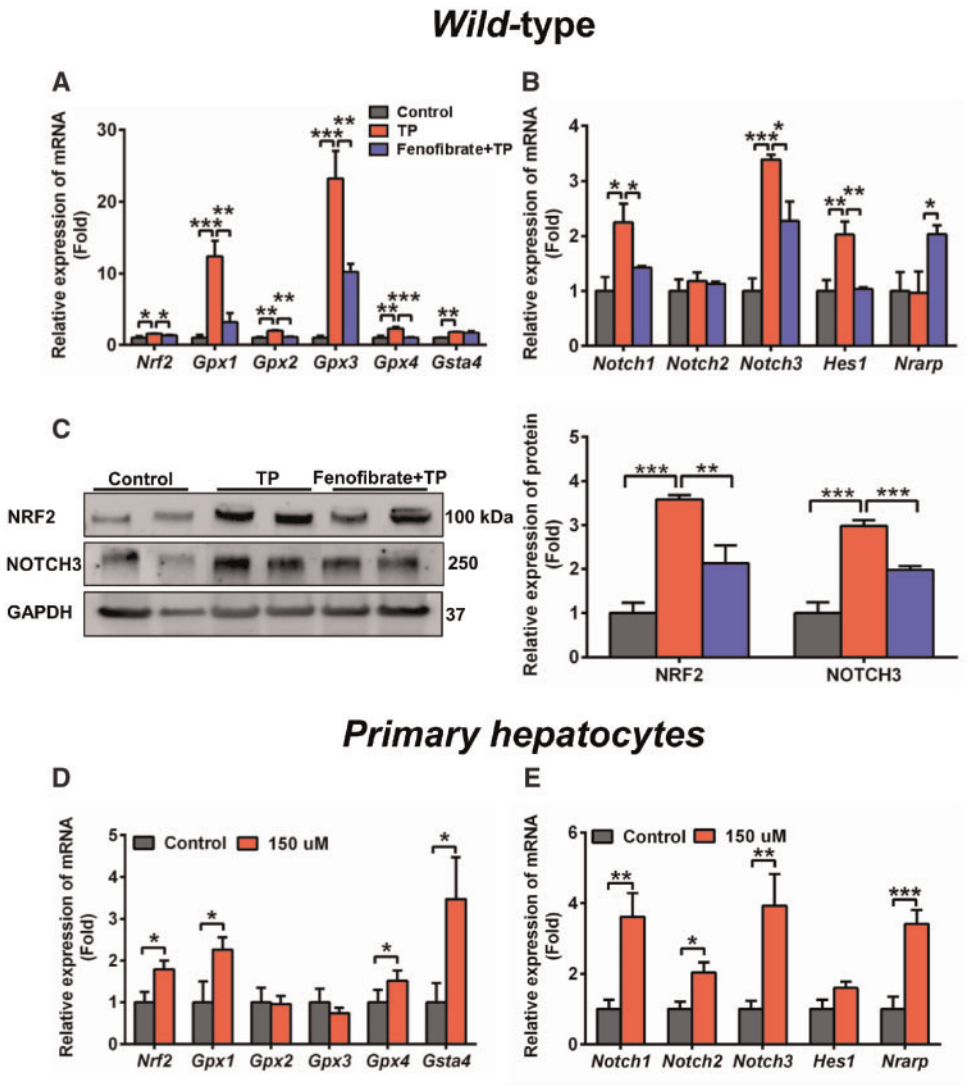

Figure 4. Long-chain acylcarnitines developed defense response by activating NRF2 and NOTCH signaling. qPCR analysis of the gene expression of NRF2 (A) and NOTCH (B) pathway in WT mice. C, Western blot was used to measure NRF2 and NOTCH3 in WT mice. qPCR analysis of the *Nrf2* (and NRF target genes) (D) and *Notch* (and NOTCH target genes) (E) mRNAs in primary hepatocytes after treatment with 150 μM 18:0-carnitine. All data were expressed as mean ± SEM. $^{*}p < .05$, $^{**}p < .01$, and $^{***}p < .001$.

α-Naphthylisothiocyanate-induced cholestasis also resulted in the accumulation of serum long-chain acylcarnitines (Zhao *et al.*, 2017). However, accumulation of long-chain acylcarnitines had not been used as a common contributing factor in liver injury even through it was known that liver injury can cause severe disruption of lipid metabolism. In this study, long-chain acylcarnitines were significantly increased in liver injury patients and TP-induced mouse liver injury models. Therefore, long-chain acylcarnitines may be a common serum biomarker for liver injury.

A previous study found that long-chain acylcarnitines had the potential to mediate a cellular stress response (McCoin *et al.*, 2015). They can activate some receptors, such as toll-like receptor 2 (TLR2), TLR4, NF-κB, cyclooxygenase-2, and JNK (McCoin *et al.*, 2015). This study demonstrated that long-chain acylcarnitines could activate the NOTCH-NRF2 pathway and induce a defense response against liver injury. This suggests that patients with increased serum levels of long-chain acylcarnitines would have a better prognosis. An earlier study revealed that tissue injury and repair were involved in hepatotoxicity (Anand and Mehendale, 2004). Therefore, some increased metabolites such as acylcarnitines, glutamine, and ursodeoxycholic acid, that appear during the process of hepatotoxicity, may have a protective role. Notably, glutamine protected against CCl_4-induced liver fibrosis, although glutamine was significantly increased in this model (Liang *et al.*, 2016; Shrestha *et al.*, 2016). Ursodeoxycholic acid, that is elevated in clinical cholestasis, is approved by the FDA to treat cholestatic liver injury (Zhao *et al.*, 2019a). Acetylcarnitine may also protect against acetaminophen-induced hepatotoxicity, although acetylcarnitine was significantly increased in this hepatotoxicity model (Alotaibi *et al.*, 2016; Bhattacharyya *et al.*, 2014; Chen *et al.*, 2009).

Peroxisome proliferator-activated receptor α is expressed in metabolically active tissues, especially liver, and regulates genes involved in lipid metabolism (Mandard *et al.*, 2004). Peroxisome proliferator-activated receptor α plays a crucial role in liver injury. The deficiency and inhibition of PPARα would aggravate liver injury. Severe liver dysfunction was induced in

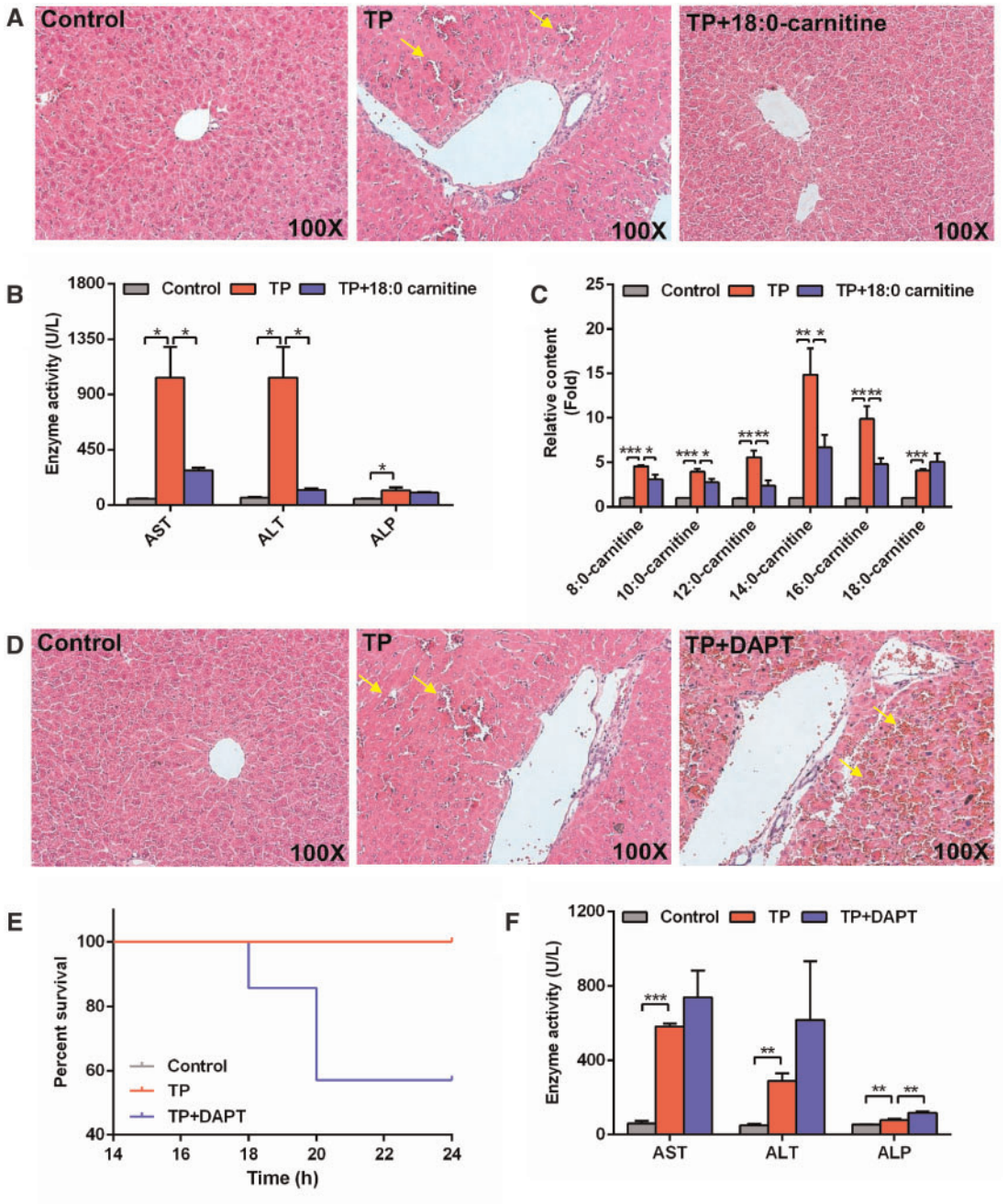

Figure 5. 18:0-Carnitine protected against TP-induced liver damage and blocked the NOTCH signaling pathway aggravated TP-induced liver damage. A, Hematoxylin and eosin staining of liver after 18:0-carnitine treatment. Solid arrow: congestion. B, Serum AST, ALT, and ALP enzymes activity after 18: 0-carnitine treatment. C, Medium- and long-chain acylcarnitine levels after 18: 0-carnitine treatment. D, Hematoxylin and eosin staining of liver after DAPT treatment. Solid arrow: congestion. E, Animal survival curves after DAPT treatment over 24 h. F, Serum AST, ALT, and ALP enzymes activity after DAPT treatment. All data were expressed as mean ± SEM. $^{*}p < .05$, $^{**}p < .01$, and $^{***}p < .001$.

Ppara−/− mice during cholic acid challenge comparing with *Ppara*+/+ mice, including disruption of bile acids, phospholipids, and cholesterol homeostasis (Li *et al.*, 2012). *Ppara*−/− mice fed a high-fat diet accumulated more hepatic triglycerides compared with *Ppara*+/+ mice (Stienstra *et al.*, 2007). Peroxisome proliferator-activated receptor α expression was lower in clinical patients with liver injury. Hepatic PPARα and CPT1α levels were profoundly lower in the patients with HCV infection compared with healthy people (Dharancy *et al.*, 2005). The level of PPARα was downregulated in alcoholic liver disease (Wan *et al.*, 1994). In humans with nonalcoholic fatty liver disease, hepatic expression of PPARα was also decreased (Francque *et al.*, 2015). Using a PPARα agonist, inhibitor, and *Ppara*−/− mice, this study provided evidence that the PPARα signaling pathway played an important role in TP-induced liver injury.

Fenofibrate is a selective PPARα agonist widely used for the treatment of hypertriglyceridemia, hyperlipidemia, and cholestatic liver disease, such as primary biliary cirrhosis (Ghonem *et al.*, 2015). Fenofibrate can improve various liver injury such as diet- or concanavalin A-induced hepatitis (Mohamed *et al.*, 2013;

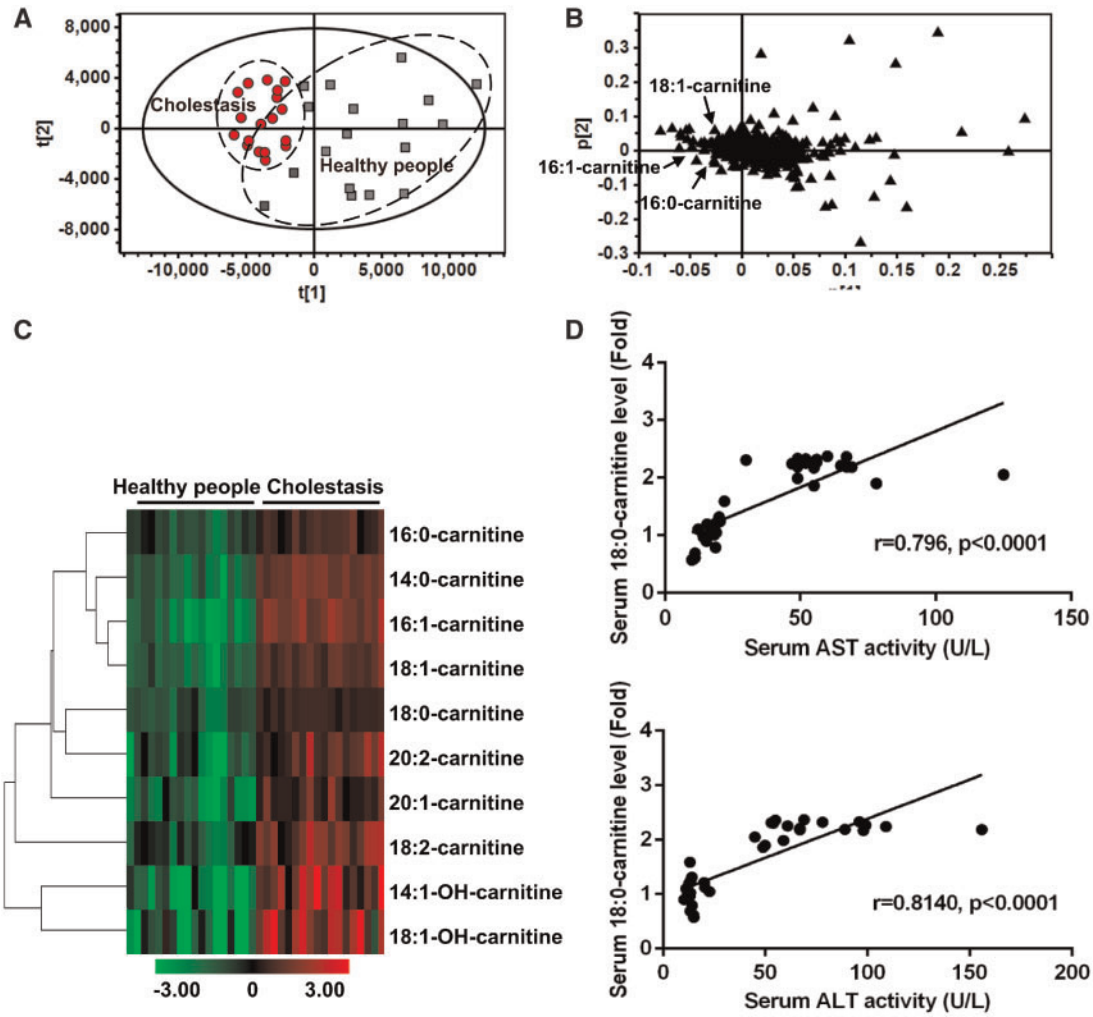

Figure 6. Long-chain acylcarnitines in cholestatic liver injury patients. Principal component analysis score plot (A) and loading plot (B) derived from UPLC-QTOFMS data of serum ions. Each point represented an individual serum sample (-left) and an ion in the sample (-right). Metabolites were labeled in the loading plot (■, Healthy people; ●, Cholestasis). C, Heat map analysis of long-chain acylcarnitines between cholestasis and healthy people. D, Correlation analysis between the levels of 18:0-carntine and serum AST and ALT. Correlation factor (*r*) and *p* value were estimated with Pearson's correlation analysis. All data were expressed as mean ± SEM.

Rajamoorthi *et al.*, 2017), hepatic ischemia reperfusion (Boshra and Moustafa, 2011), cholestasis (Zhao *et al.*, 2017), and sunitinib-induced hepatic injury (Zhao *et al.*, 2019b). This study demonstrated that fenofibrate could protect TP-induced liver injury in animal models.

NOTCH signaling is an intracellular signaling pathway, related to liver injury that result from drug-induced hepatotoxicity, inflammation, hepatic ischemia reperfusion, and liver fibrosis (Bansal *et al.*, 2015; Jiang *et al.*, 2017; Wei *et al.*, 2016; Yu *et al.*, 2016). A previous study reported that TP treatment increased NOTCH signaling (Wang *et al.*, 2016). Furthermore, NRF2-related genes could be upregulated by 16:0-carnitine (Zhao *et al.*, 2017). NRF2 is a transcription factor that mediates a broad-based set of adaptive responses to cellular stresses (Wakabayashi *et al.*, 2010), and is closely related to various liver diseases, including cholestasis, drug-induced hepatotoxicity, hepatic ischemia reperfusion, and hepatic iron overload (Kudoh *et al.*, 2014; Silva-Gomes *et al.*, 2014; Zollner *et al.*, 2010). Therefore, NOTCH-NRF2 signaling is important in hepatoprotection. Both NOTCH and NRF2 are evolutionarily conserved among animals, and there exists transcriptional cross-talk between the NOTCH and NRF2 pathways. NOTCH signaling could directly activate NRF2 through combination of the NICD transcriptosome to the *Nrf2* promoter (Wakabayashi *et al.*, 2014). NRF2 can also directly regulate NOTCH signaling through an antioxidant response element sequences in the *Notch* promoter (Wakabayashi *et al.*, 2010). In this study, NOTCH-NRF2 signaling was significantly activated by TP in murine models, which induced defense response.

PPARα signaling was significantly inhibited in TP-induced liver injury. Peroxisome proliferator-activated receptor α activation by fenofibrate markedly improved TP-induced liver injury, whereas PPARα inhibition by the antagonist GW6471 potentiated liver injury, indicating an important role for PPARα in the hepatoprotection. Increased long-chain acylcarnitines were further found to protect against TP-induced liver injury. These findings provide the evidence for the protective role of PPARα and long-chain acylcarnitines in TP-induced hepatotoxicity, and suggested that the modulation of PPARα may protect against clinical liver injury.

SUPPLEMENTARY DATA

Supplementary data are available at *Toxicological Sciences* online.

DECLARATION OF CONFLICTING INTERESTS

The authors declared no potential conflicts of interest with respect to the research, authorship, and/or publication of this article.

FUNDING

This work was supported by the National Key Research and Development Program of China (2017YFC1700906, 2017YFC0906903); CAS "Light of West China" Program (Y72E8211W1); Kunming Institute of Botany (Y76E1211K1, Y4662211K1); and State Key Laboratory of Phytochemistry and Plant Resources in West China (52Y67A9211Z1).

REFERENCES

Alotaibi, S. A., Alanazi, A., Bakheet, S. A., Alharbi, N. O., and Nagi, M. N. (2016). Prophylactic and therapeutic potential of acetyl-L-carnitine against acetaminophen-induced hepatotoxicity in mice. *J. Biochem. Mol. Toxicol.* **30**, 5–11.

Anand, S. S., and Mehendale, H. M. (2004). Liver regeneration: A critical toxicodynamic response in predictive toxicology. *Environ. Toxicol. Pharmacol.* **18**, 149–160.

Bansal, R., van Baarlen, J., Storm, G., and Prakash, J. (2015). The interplay of the Notch signaling in hepatic stellate cells and macrophages determines the fate of liver fibrogenesis. *Sci. Rep.* **5**, 18272.

Bhattacharyya, S., Yan, K., Pence, L., Simpson, P. M., Gill, P., Letzig, L. G., Beger, R. D., Sullivan, J. E., Kearns, G. L., and Reed, M. D. (2014). Targeted liquid chromatography-mass spectrometry analysis of serum acylcarnitines in acetaminophen toxicity in children. *Biomarkers Med.* **8**, 147–159.

Bhushan, B., Poudel, S., Manley, M. W., Jr, Roy, N., and Apte, U. (2017). Inhibition of glycogen synthase kinase 3 accelerated liver regeneration after acetaminophen-induced hepatotoxicity in mice. *Am. J. Pathol.* **187**, 543–552.

Bhushan, B., Walesky, C., Manley, M., Gallagher, T., Borude, P., Edwards, G., Monga, S. P., and Apte, U. (2014). Pro-regenerative signaling after acetaminophen-induced acute liver injury in mice identified using a novel incremental dose model. *Am. J. Pathol.* **184**, 3013–3025.

Boshra, V., and Moustafa, A. M. (2011). Effect of preischemic treatment with fenofibrate, a peroxisome proliferator-activated receptor-α ligand, on hepatic ischemia-reperfusion injury in rats. *J. Mol. Histol.* **42**, 113–122.

Chen, C., Krausz, K. W., Shah, Y. M., Idle, J. R., and Gonzalez, F. J. (2009). Serum metabolomics reveals irreversible inhibition of fatty acid β-oxidation through the suppression of PPARα activation as a contributing mechanism of acetaminophen-induced hepatotoxicity. *Chem. Res. Toxicol.* **22**, 699–707.

Chen, D. Q., Cao, G., Chen, H., Liu, D., Su, W., Yu, X. Y., Vaziri, N. D., Liu, X. H., Bai, X., and Zhang, L. (2017). Gene and protein expressions and metabolomics exhibit activated redox signaling and wnt/β-catenin pathway are associated with metabolite dysfunction in patients with chronic kidney disease. *Redox Biol.* **12**, 505–521.

Chen, H., Cao, G., Chen, D. Q., Wang, M., Vaziri, N. D., Zhang, Z. H., Mao, J. R., Bai, X., and Zhao, Y. Y. (2016). Metabolomics insights into activated redox signaling and lipid metabolism dysfunction in chronic kidney disease progression. *Redox Biol.* **10**, 168–178.

Crespillo, A., Alonso, M., Vida, M., Pavon, F. J., Serrano, A., Rivera, P., Romero-Zerbo, Y., Fernandez-Llebrez, P., Martinez, A., and Perez-Valero, V. (2011). Reduction of body weight, liver steatosis and expression of stearoyl-CoA desaturase 1 by the isoflavone daidzein in diet-induced obesity. *Br. J. Pharmacol.* **164**, 1899–1915.

Dharancy, S., Malapel, M., Perlemuter, G., Roskams, T., Cheng, Y., Dubuquoy, L., Podevin, P., Conti, F., Canva, V., Philippe, D., *et al.* (2005). Impaired expression of the peroxisome proliferator-activated receptor α during hepatitis C virus infection. *Gastroenterology* **128**, 334–342.

Francque, S., Verrijken, A., Caron, S., Prawitt, J., Paumelle, R., Derudas, B., Lefebvre, P., Taskinen, M. R., Van Hul, W., Mertens, I., *et al.* (2015). PPARα gene expression correlates with severity and histological treatment response in patients with non-alcoholic steatohepatitis. *J. Hepatol.* **63**, 164–173.

Ghonem, N. S., Assis, D. N., and Boyer, J. L. (2015). Fibrates and cholestasis. *Hepatology* **62**, 635–643.

Gongora, L., Manez, S., Giner, R. M., Recio, M. C., and Rios, J. L. (2000). On the activity of trifluoperazine and palmitoylcarnitine in mice: Delayed hypersensitivity models. *Life Sci.* **66**, Pl183–188.

Hu, D. D., Chen, X. L., Xiao, X. R., Wang, Y. K., Liu, F., Zhao, Q., Li, X., Yang, X. W., and Li, F. (2018). Comparative metabolism of tripolide and triptonide using metabolomics. *Food Chem. Toxicol.* **115**, 98–108.

Jiang, L., Ke, M., Yue, S., Xiao, W., Yan, Y., Deng, X., Ying, Q. L., Li, J., and Ke, B. (2017). Blockade of Notch signaling promotes acetaminophen-induced liver injury. *Immunol. Res.* **65**, 739–749.

Kudoh, K., Uchinami, H., Yoshioka, M., Seki, E., and Yamamoto, Y. (2014). Nrf2 activation protects the liver from ischemia/reperfusion injury in mice. *Ann. Surg.* **260**, 118–127.

Li, F., Patterson, A. D., Krausz, K. W., Tanaka, N., and Gonzalez, F. J. (2012). Metabolomics reveals an essential role for peroxisome proliferator-activated receptor α in bile acid homeostasis. *J. Lipid Res.* **53**, 1625–1635.

Li, F., Yang, X. W., Krausz, K. W., Nichols, R. G., Xu, W., Patterson, A. D., and Gonzalez, F. J. (2015). Modulation of colon cancer by nutmeg. *J. Proteome Res.* **14**, 1937–1946.

Liang, Y. H., Tang, C. L., Lu, S. Y., Cheng, B., Wu, F., Chen, Z. N., Song, F., Ruan, J. X., Zhang, H. Y., Song, H., *et al.* (2016). Serum metabonomics study of the hepatoprotective effect of *Corydalis saxicola* Bunting on carbon tetrachloride-induced acute hepatotoxicity in rats by (1)H NMR analysis. *J. Pharm. Biomed. Anal.* **129**, 70–79.

Liu, J., Wu, Q. L., Feng, Y. H., Wang, Y. F., Li, X. Y., and Zuo, J. P. (2005). Triptolide suppresses CD80 and CD86 expressions and IL-12 production in THP-1 cells. *Acta Pharmacol. Sin.* **26**, 223–227.

Mandard, S., Muller, M., and Kersten, S. (2004). Peroxisome proliferator-activated receptor α target genes. *Cell. Mol. Life Sci.* **61**, 393–416.

Matlin, S. A., Belenguer, A., Stacey, V. E., Qlan, S. Z., Xu, Y., Zhang, J. W., Sanders, J. K. M., Amor, S. R., and Pearce, C. M. (1993). Male antifertility compounds from *Tripterygium wilfordii* Hook F. *Contraception* **47**, 387–400.

McCoin, C. S., Knotts, T. A., and Adams, S. H. (2015). Acylcarnitines—Old actors auditioning for new roles in metabolic physiology. *Nat. Rev. Endocrinol.* **11**, 617–625.

McGill, M. R., Li, F., Sharpe, M. R., Williams, C. D., Curry, S. C., Ma, X. C., and Jaeschke, H. (2014). Circulating acylcarnitines as biomarkers of mitochondrial dysfunction after acetaminophen overdose in mice and humans. *Arch. Toxicol.* **88**, 391–401.

Mohamed, D. I., Elmelegy, A. A., El-Aziz, L. F., Abdel Kawy, H. S., El-Samad, A. A., and El-Kharashi, O. A. (2013). Fenofibrate A peroxisome proliferator activated receptor-α agonist treatment ameliorates concanavalin A-induced hepatitis in rats. *Eur. J. Pharmacol.* **721**, 35–42.

Primassin, S., Ter Veld, F., Mayatepek, E., and Spiekerkoetter, U. (2008). Carnitine supplementation induces acylcarnitine production in tissues of very long-chain acyl-CoA dehydrogenase-deficient mice, without replenishing low free carnitine. *Pediatr. Res.* **63**, 632–637.

Rajamoorthi, A., Arias, N., Basta, J., Lee, R. G., and Baldan, A. (2017). Amelioration of diet-induced steatohepatitis in mice following combined therapy with ASO-Fsp27 and fenofibrate. *J. Lipid Res.* **58**, 2127–2138.

Santra, S., and Hendriksz, C. (2010). How to use acylcarnitine profiles to help diagnose inborn errors of metabolism. *Arch. Dis. Child Educ.* **95**, 151–156.

Shi, X. L., Yao, D., Gosnell, B. A., and Chen, C. (2012). Lipidomic profiling reveals protective function of fatty acid oxidation in cocaine-induced hepatotoxicity. *J. Lipid Res.* **53**, 2318–2330.

Shrestha, N., Chand, L., Han, M. K., Lee, S. O., Kim, C. Y., and Jeong, Y. J. (2016). Glutamine inhibits CCl_4 induced liver fibrosis in mice and TGF-β1 mediated epithelial-mesenchymal transition in mouse hepatocytes. *Food Chem. Toxicol.* **93**, 129–137.

Silva-Gomes, S., Santos, A. G., Caldas, C., Silva, C. M., Neves, J. V., Lopes, J., Carneiro, F., Rodrigues, P. N., and Duarte, T. L. (2014). Transcription factor NRF2 protects mice against dietary iron-induced liver injury by preventing hepatocytic cell death. *J. Hepatol.* **60**, 354–361.

Soga, T., Sugimoto, M., Honma, M., Mori, M., Igarashi, K., Kashikura, K., Ikeda, S., Hirayama, A., Yamamoto, T., Yoshida, H., *et al.* (2011). Serum metabolomics reveals gamma-glutamyl dipeptides as biomarkers for discrimination among different forms of liver disease. *J. Hepatol.* **55**, 896–905.

Stienstra, R., Mandard, S., Patsouris, D., Maass, C., Kersten, S., and Müller, M. (2007). Peroxisome proliferator-activated receptor α protects against obesity-induced hepatic inflammation. *Endocrinology* **148**, 2753–2763.

Tao, X., Cush, J. J., Garret, M., and Lipsky, P. E. (2001). A phase I study of ethyl acetate extract of the Chinese antirheumatic herb *Tripterygium wilfordii* Hook F in rheumatoid arthritis. *J. Rheumatol.* **28**, 2160–2167.

Wakabayashi, N., Chartoumpekis, D. V., and Kensler, T. W. (2015). Crosstalk between Nrf2 and Notch signaling. *Free Radic. Biol. Med.* **88**, 158–167.

Wakabayashi, N., Skoko, J. J., Chartoumpekis, D. V., Kimura, S., Slocum, S. L., Noda, K., Palliyaguru, D. L., Fujimuro, M., Boley, P. A., Tanaka, Y., *et al.* (2014). Notch-Nrf2 axis: Regulation of Nrf2 gene expression and cytoprotection by notch signaling. *Mol. Cell. Biol.* **34**, 653–663.

Wakabayashi, N., Slocum, S. L., Skoko, J. J., Shin, S., and Kensler, T. W. (2010). When NRF2 talks, who's listening? *Antioxid. Redox Signal.* **13**, 1649–1663.

Wan, Y. J., Morimoto, M., Thurman, R. G., Bojes, H. K., and French, S. W. (1994). Expression of the peroxisome proliferator-activated receptor gene is decreased in experimental alcoholic liver disease. *Life Sci.* **56**, 307–317.

Wang, X., Sun, L., Zhang, L., and Jiang, Z. (2016). Effect of adoptive transfer or depletion of regulatory T cells on triptolide-induced liver injury. *Front. Pharmacol.* **7**, 99.

Wei, X., Wang, J. P., Hao, C. Q., Yang, X. F., Wang, L. X., Huang, C. X., Bai, X. F., Lian, J. Q., and Zhang, Y. (2016). Notch signaling contributes to liver inflammation by regulation of interleukin-22-producing cells in hepatitis B virus infection. *Front. Cell. Infect. Microbiol.* **6**, 132.

Yaligar, J., Teoh, W. W., Othman, R., Verma, S. K., Phang, B. H., Lee, S. S., Wang, W. W., Toh, H. C., Gopalan, V., and Sabapathy, K. (2016). Longitudinal metabolic imaging of hepatocellular carcinoma in transgenic mouse models identifies acylcarnitine as a potential biomarker for early detection. *Sci. Rep.* **6**, 20299.

Yang, S., Chen, J., Guo, Z., Xu, X. M., Wang, L., Pei, X. F., Yang, J., Underhill, C. B., and Zhang, L. (2003). Triptolide inhibits the growth and metastasis of solid tumors. *Mol. Cancer Ther.* **2**, 65–72.

Yu, H. C., Bai, L., Yang, Z. X., Qin, H. Y., Tao, K. S., Han, H., and Dou, K. F. (2016). Blocking Notch signal in myeloid cells alleviates hepatic ischemia reperfusion injury by repressing the activation of NF-kappaB through CYLD. *Sci. Rep.* **6**, 32226.

Zhang, Y., Li, F., Patterson, A. D., Wang, Y., Krausz, K. W., Neale, G., Thomas, S., Nachagari, D., Vogel, P., Vore, M., *et al.* (2012). Abcb11 deficiency induces cholestasis coupled to impaired β-fatty acid oxidation in mice. *J. Biol. Chem.* **287**, 24784–24794.

Zhao, Q., Liu, F., Cheng, Y., Xiao, X. R., Hu, D. D., Tang, Y. M., Bao, W. M., Yang, J. H., Jiang, T., Hu, J. P., *et al.* (2019a). Celastrol protects from cholestatic liver injury through modulation of SIRT1-FXR signaling. *Mol. Cell. Proteomics* **18**, 520–533.

Zhao, Q., Yang, R., Wang, J., Hu, D. D., and Li, F. (2017). PPARα activation protects against cholestatic liver injury. *Sci. Rep.* **7**, 9967.

Zhao, Q., Zhang, J. L., and Li, F. (2018). Application of metabolomics in the study of natural products. *Nat. Prod. Bioprospect.* **8**, 321–334.

Zhao, Q., Zhang, T., Xiao, X. R., Huang, J. F., Wang, Y., Gonzalez, F. J., and Li, F. (2019b). Impaired clearance of sunitinib leads to metabolic disorders and hepatotoxicity. *Br. J. Pharmacol.* **176**, 2162–2178.

Zollner, G., Wagner, M., and Trauner, M. (2010). Nuclear receptors as drug targets in cholestasis and drug-induced hepatotoxicity. *Pharmacol. Ther.* **126**, 228–243.